Biogeosciences Discuss., 11, 7273–7290, 2014
www.biogeosciences-discuss.net/11/7273/2014/
doi:10.5194/bgd-11-7273-2014

Biogeosciences Discussions
Open Access

Role of extracellular polymeric substances (EPS) from *Pseudomonas putida* strain MnB1 in dissolution of natural rhodochrosite

H. Wang[1,2] **and X. Pan**[1]

[1]Laboratory of Environmental Pollution and Bioremediation, State Key Laboratory of Desert and Oasis Ecology, Xinjiang Institute of Ecology and Geography, Chinese Academy of Sciences, Urumqi 830011, China
[2]University of Chinese Academy of Sciences, Beijing, 100049, China

Received: 16 April 2014 – Accepted: 9 May 2014 – Published: 20 May 2014

Correspondence to: X. Pan (panxl@ms.xjb.ac.cn)

Published by Copernicus Publications on behalf of the European Geosciences Union.

Abstract

Microbially mediated oxidation of Mn(II) to Mn oxides have been demonstrated in previous studies, however, the mechanisms of bacteria how to dissolve and oxidize using a solid Mn(II) origin are poorly understood. In this study, we examined the role of extracellular polymeric substances (EPS) from *P. putida* strain MnB1 in enhancing dissolution of natural rhodochrosite. The results showed that *P. putida* strain MnB1 cell can effectively dissolve and oxidize natural rhodochrosite to generate Mn oxides, and EPS were found to play an important role in increasing dissolution of natural rhodochrosite. Compared with EPS-free treatment, dissolution rate of natural rhodochrosite in the presence of bacterial EPS was significantly increased with decreasing initial pH and increasing EPS concentration, ionic strength and rhodochrosite dosage ($p < 0.05$). The fourier-transform infrared spectroscopy (FTIR) analysis implies that the functional groups like N-H, C=O and C-H in EPS contributed to the dissolution of natural rhodochrosite. This study is helpful for understanding the mechanisms of the formation of biogenic Mn oxides using a solid Mn(II) origin.

1 Introduction

Mn oxides are thought to be one of the most important minerals in surface waters (Shiller and Stephens, 2005; Tebo et al., 2005). These Mn oxides are of importance in the cycling of nutrients elements, the transformation of toxic persistent pollutants and the detainment of heavy metals because of their high reactivity and wide existence in the environments (Tebo et al., 2005; Zhu et al., 2009; Lafferty et al., 2010). Since 1960s, microbially mediated oxidation of divalent Mn ion to generate Mn oxides was reported, and some relevant mechanisms of Mn oxidation induced by the microbes have been illustrated recently (Villalobos et al., 2003; Spiro et al., 2010; Learman et al., 2011a, b; Hansel et al., 2012). Rhodochrosite ($MnCO_3$) was a solid Mn(II) origin mineral and the

BGD
11, 7273–7290, 2014

deposit of natural rhodochrosite was widely distributed (Germann, 1973; Okita, 1992; Roy, 1997; Fan and Yang, 1999).

Oxidative dissolution of rhodochrosite leads to produce dissociative Mn(II) and Mn oxides. The solubility of synthetic rhodochrosite in pure water and saline solution has been reported, meanwhile, rhodochrosite oxidation by O_2 or iron oxides is thermodynamically favorable, but the oxidation rate is rather slow (Diem and Stumm, 1984; Jensen et al., 2002; Luo and Millero, 2003; Duckworth and Martin, 2004; Madden and Hochella, 2005). Recently, oxidative dissolution of natural rhodochrosite by fungi has been reported (Tang et al., 2013). However, the mechanism of natural rhodochrosite dissolution induced by the microbes has not been well demonstrated. For example, to our knowledge, the information about the bacteria how to use natural rhodochrosite is limited.

Oxidative dissolution of natural rhodochrosite by the microbes may link to a dynamic process at solid–liquid interfaces. For example, the bio-leaching of metal sulfides minerals were mediated by a series of interfacial processes such as attachment of cell to surfaces of minerals, dissolution of mineral by bacterial EPS and oxidation of low valence Fe and S (Bosecker, 1997; Gehrke et al., 1998; Fowler et al., 1999; Tributsch, 2001; Rohwerder et al., 2003). Until now, the mechanism of bio-leaching in some aspects is still open questions for the researchers. Therefore, studying the interfacial processes at bacterial EPS layer and rhodochrosite mineral surface is helpful to understand the mechanism of bacterial oxidation of solid origin Mn(II) and the biogeochemical cycles of Mn.

In this study, the role of EPS in oxidative dissolution of natural rhodochrosite was investigated using a Mn oxidizing bacterium, *Pseudomonas putida* MnB1. The dissolution and oxidation kinetics of rhodochrosite was examined by batch experiments and the products of Mn oxides were checked through the scanning electron microscope and energy dispersive spectrometer (SEM-EDS) analysis. Moreover, effects of pH, EPS concentration, ion strength and rhodochrosite dosage on dissolution rate of

BGD
11, 7273–7290, 2014

rhodochrosite in the presence of EPS were also investigated. The functional groups in EPS involved in dissolving rhodochrosite were analyzed by FTIR.

2 Materials and methods

2.1 Culture of bacterium

The Mn oxidizing bacterium *P. putida* strain MnB1 (ATCC 23483) was used in this study. The *P. putida* MnB1 cells was cultured in the medium under aerobic conditions reported by Kim et al. (2012), which was composed of 0.5 g L^{-1} of yeast extract, 1 g L^{-1} of glucose, 0.5 g L^{-1} of casamino acids, 0.815 g L^{-1} $MgSO_4 \cdot 7H_2O$, 0.294 g L^{-1} of $CaCl_2 \cdot 2H_2O$, 0.001 g L^{-1} $FeCl_3 \cdot 7H_2O$ and 1 mL of trace element solution. The trace element solution was composed of 2.496 g L^{-1} $CuSO_4 \cdot 5H_2O$, 12.653 g L^{-1} $ZnSO_4 \cdot 7H_2O$, 4.758 g L^{-1} $CoCl_2 \cdot 6H_2O$ and 3.145 g L^{-1} $Na_2MoO_4 \cdot 2H_2O$. The cells were harvested after two days of culture for further experiments. For batch experiments, *P. putida* MnB1 was incubated at 25 °C in the #279 medium (ATCC™) containing 0.15 g of $Fe(NH_4)_2(SO_4)_2 \cdot 6H_2O$, 0.075 g of yeast extract, 0.15 g of sodium citrate, 0.05 g of $Na_4P_2O_7 \cdot 10H_2O$ in one liter of Milli-Q water with an initial pH of 6.8.

2.2 Preparation of rhodochrosite

Natural rhodochrosite mineral was collected from a Mn mine near Xiangtan city, Hunan province, China. The mineral samples were dried at ambient temperature and grinded through 0.15 mm nylon screen. Prior to the batch experiments, the samples were washed three times by Milli-Q water to remove the dissociative Mn(II). X ray diffraction (XRD) analysis shows that the raw mineral mainly contains rhodochrosite and some quartz (Fig. 1) with a total Mn content of 201.93 ± 11.42 mg g^{-1}.

BGD
11, 7273–7290, 2014

2.3 Oxidative dissolution of rhodochrosite by *P. putida* MnB1

Experiments about oxidation dissolution of rhodochrosite by *P. putida* MnB1 were carried out in 100 mL glass bottles with rubber stopper. About 50 mL of fresh sterilized medium and 0.2 g of natural rhodochrosite were added into the glass bottles containing bacterial cell suspension at a density of 4×10^7 cellsmL^{-1}. Inactivated control was performed using Na_3N treatment (0.3 %, wt) to inhibit the biological activity of *P. putida* MnB1. The bottles without cells were used as the sterile control. All the treatments were done in triplicate. The bottles were shaken at 120 rpm and 25 °C. At different time intervals, aliquots of samples were collected and centrifuged at 12 000 rpm for 5 min. Concentration of Mn(II) in supernatant was measured. The residues were re-suspended in Milli-Q water for Mn oxides analysis.

2.4 Dissolution of natural rhodochrosite by bacterial EPS

For EPS extraction, cells were grown in the medium at 120 rpm and 25 °C for 3 days (OD_{600} = 0.8). The method for EPS extraction was slightly modified based on a previous report (Zhang et al., 2013). Briefly, the cell samples were centrifuged at 8000 rpm for 5 min at 4 °C to remove superfluous medium. The residues were re-suspended in Milli-Q water and centrifuged at 18 000 rpm for 25 min at 4 °C. The suspension was collected and filtered through 0.45 µm acetate cellulose membrane and further purified with 3500 Dalton dialysis membrane for 5 times at 4 °C in the dark. The EPS samples of *P. putida* MnB1 had the following characteristics: TOC, 51 ± 1.52 mg L^{-1}; proteins, 47.03 ± 0.22 µg mL^{-1}; polysaccharides, 11.12 ± 0.04 µg mL^{-1}; and pH 6.8. In addition, the freeze dried EPS was stored at −20 °C in the dark for further experiments.

The experiments of dissolution of natural rhodochrosite by EPS were done in 50 mL Erlenmeyer flasks on a reciprocating shaker at 200 rpm and 25 °C. Effects of environmental factors, such as pH, ionic strength, EPS concentration and rhodochrosite dosage were examined. The treatment without addition of EPS was set as the control. The experimental parameters of natural rhodochrosite dissolution rate for different

BGD
11, 7273–7290, 2014

treatments were summarized in Table 1. The pH of all test solution was adjusted by 0.01 M NaOH or HCl and measured by an automatic potentiometric titrator with a pH electrode (Metrohm 702, Switzerland). Different ionic strength was obtained by addition of different amount of NaCl. After 360 min reaction, samples were collected and filtered through 0.22 μm filters for Mn(II) analysis. Each experiment was conducted in triplicate.

2.5 Analytical methods

Mn(II) concentration in solution was measured by the manganese formaldehyde oxime spectrophotometry (Brewer and Spencer, 1971). Content of biogenic Mn oxides was determined according to the Leukoberbelin blue (LBB) colorimetrical method (Okazaki et al., 1997). The standard curves were obtained by oxidation of LBB by $KMnO_4$ and the data were shown as MnO_2 equivalents. The content of TOC in EPS samples was determined by a TOC analyzer (Model 1030, Aurora, USA). The polysaccharides content in EPS was determined by the phenol–sulfuric acid method (Saha and Brewer, 1994). Content of proteins in EPS was measured using the modified Lowry procedure (Paxman, 1972).

For SEM-EDS, XRD and FTIR analysis, the samples were lyophilized by a vacuum freeze dryer. The FTIR analysis of EPS samples were recorded using a FTIR spectrophotometer (Vertex 70, Bruker, Germany). The Mn oxides samples were sprayed with gold and analyzed by SEM (Zeiss Super 55VP, Germany) coupled with EDS spectroscopy (Bruker XFlash 5010, Germany). XRD spectrum was obtained by an X-ray diffractometer (Bruker D8, Germany).

3 Results and discussion

3.1 Oxidative dissolution of rhodochrosite by *P. putida* MnB1

Oxidative dissolution of natural rhodochrosite by live *P. putida* MnB1 resulted in the formation of biogenic Mn oxides and the removal of Mn(II) from solution (Figs. 2 and

BGD
11, 7273–7290, 2014

3). The Mn oxides produced by *P. putida* MnB1 and freshly synthetic δ-MnO_2 were analyzed by SEM-EDS (Fig. 2). The SEM graphs showed that cells were adhered to the surface of Mn oxides and the biogenic Mn oxides were composed of poorly order, poorly crystalline phyllomanganate, similar to δ-MnO_2. This is consistent with the previous studies (Villalobos et al., 2003). The EDS analysis showed that the biogenic and synthetic Mn oxides were mainly composed of O and Mn, and other elements, such as Fe, P and Mg, were originated from the culture medium.

The LBB tests also supported the oxidation of Mn(II) (Fig. 3a). In the sterile control and the inactivated control, the oxidation rates of natural rhodochrosite was rather slow or inhibited, which indicates that abiotic oxidation process is thermodynamically favorable but at a rather low rate (Diem and Stumm, 1984). On the contrary, the presence of *P. putida* MnB1 caused a significant increase in Mn oxides content with the reaction time ($p < 0.05$). For example, after reaction from 1 d to 7 d onset of experiments, Mn oxides content increased from $6.28 \pm 0.42\,mg\,L^{-1}$ to $22.31 \pm 5.31\,mg\,L^{-1}$.

Figure 3b illustrated the changes of dissolved Mn(II) concentration during reaction of *P. putida* MnB1 with natural rhodochrosite. Mn(II) concentration was significantly lower for live *P. putida* MnB1 treatment than the sterile control and the inactivated control ($p < 0.05$). For example, over the entire reaction time, dissolved Mn(II) released from the natural rhodochrosite was kept in less than $0.5\,mg\,L^{-1}$ in the presence of live cells, while Mn(II) concentration was significantly increased for the inactivated cell treatment ($p < 0.05$). This means that live cell can effectively oxidize Mn^{2+} in solution to form Mn oxides. The dissolution rate of natural rhodochrosite may be determined by the mineral forms of rhodochrosite or other environmental factors. Moreover, abiotic dissolution of natural rhodochrosite caused release of dissolved Mn(II) (Fig. 3) (Jensen et al., 2002; Luo and Millero, 2003). Overall, when comparing to Fig. 3a and b, we can find that only live cell can directly dissolve and oxidize natural rhodochrosite to produce Mn oxides, while inactivated cell treatment or cell-free treatment did not contribute to the formation of Mn oxides.

BGD
11, 7273–7290, 2014

3.2 Dissolution of natural rhodochrosite by bacterial EPS

The dissolution rate of natural rhodochrosite at various pHs, ionic strengths, EPS concentrations and rhodochrosite dosages with and without bacterial EPS were listed in Table 1. The dissolution rate of natural rhodochrosite by EPS was significantly increased at low pH condition ($p < 0.05$) in comparison with the EPS-free treatment. For example, when solution pH decreased from 8.0 to 5.0, the dissolution rate for control treatment was only increased about 1.2 times, but in the presence EPS, the rate was increased by more than 26 times. This might be attributed to consumption of H^+ ions required by the dissolution of $MnCO_3$ (Duckworth and Martin, 2004). Moreover, the dissolution rate was increased with EPS concentration under neutral conditions (pH = 7.0). The dissolution rates were 0.055 ± 0.003, 0.075 ± 0.003 and 0.111 ± 0.018 μg Mn(II) min^{-1} for EPS concentrations of 0, 0.4 and 1.6 mg TOC L^{-1}, respectively. High levels of ionic strength (0.1 and 0.5 M NaCl) increased Mn(II) concentration in the presence of 0.8 mg TOC L^{-1} EPS, and the dissolution rate increased by 15.6 % as ionic strength increased from 0.1 to 0.5 mol L^{-1}. For EPS treatment, dissolution rate of natural rhodochrosite was also increased with the rhodochrosite dosage. In addition, EPS did not show the ability to oxidize Mn^{2+} to Mn oxides during 5 d reaction (data not shown). These results indicate that bacterial EPS contributed to the increasing dissolution of natural rhodochrosite, which was influenced by water chemistry factors, such as pH, EPS concentration and ionic strength. This suggests that EPS secreted by *P. putida* MnB1 cell play a significant role in enhancing the dissolution of natural rhodochrosite and subsequent release of Mn(II) for bacterial Mn oxidation ($p < 0.05$).

3.3 Dissolution mechanism of natural rhodochrosite identified by FTIR

Oxidative dissolution of natural rhodochrosite to produce Mn oxides by fungi was reported (Tang et al., 2013), however, little is known about the reaction mechanism of EPS involved in dissolution of natural rhodochrosite. Functional groups of bacterial EPS

BGD
11, 7273–7290, 2014

involved in dissolution of natural rhodochrosite were explored by FTIR analysis (Fig. 4). For the purified EPS, the band at 3422 cm^{-1} is attributed to O-H stretching in polysaccharides or protein groups and the band at 2931 cm^{-1} corresponded to C-H stretching (Braissant et al., 2007). The band at 1653 cm^{-1} is ascribed to the C=O stretching in amide I, while the band at 1541 cm^{-1} is attributable to N-H bending in proteins (Guibaud et al., 2003, 2005). The band near 1400 cm^{-1} is ascribed to the symmetric stretching of C=O in COOH and the band at 1241 cm^{-1} is ascribed to N-H bending and C-N stretching vibrations (Nara et al., 1994; Omoike and Chorover, 2004). The band at 1038 cm^{-1} is mainly attributed to the stretching of C-O-C and C-H in polysaccharides (Guibaud et al., 2005; Comte et al., 2006). After reaction of natural Rhodochrosite, the bands at 1241 cm^{-1} and 1541 cm^{-1} disappeared, whereas the bands near 1653 cm^{-1} and 1400 cm^{-1} became much weaker. Besides, the bands near 2931 cm^{-1} and 1083 cm^{-1} became a doublet located at 2938 cm^{-1} and 2885 cm^{-1}, 1110 cm^{-1} and 1046 cm^{-1}, respectively. Overall, these results suggest that the functional groups of N-H in proteins, C=O in COOH or amide I and C-H or C-O-C in polysaccharides are directly involved in the dissolution of natural rhodochrosite.

4 Conclusions

In this study, the results showed that *P. putida* strain MnB1 cell can effectively oxidize and dissolve the natural rhodochrosite to produce Mn oxides, and EPS from bacteria played an important role in enhancing the dissolution of rhodochrosite by *P. putida* strain MnB1. Dissolution rate of natural rhodochrosite in the presence of EPS was significantly enhanced under acidic condition, and other factors such as EPS concentration, ionic strength and rhodochrosite dosage also significantly affected dissolution of natural rhodochrosite. FTIR analysis indicated that the dissolution of natural rhodochrosite by EPS was mainly attributed to the involvement of N-H, C=O and C-H groups. This study for the first time demonstrated the important role of bacterial EPS in biotic dissolution and oxidation of natural rhodochrosite.

BGD
11, 7273–7290, 2014

Acknowledgement. This work was supported by the National Natural Science Foundation of China (U1120302 and 21177127).

References

Bosecker, K.: Bioleaching: metal solubilization by microorganisms, Fems Microbiol. Rev., 20, 591–604, doi:10.1111/j.1574-6976.1997.tb00340.x, 1997.

Braissant, O., Decho, A. W., Dupraz, C., Glunk, C., Przekop, K. M., and Visscher, P. T.: Exopolymeric substances of sulfate-reducing bacteria: interactions with calcium at alkaline pH and implication for formation of carbonate minerals, Geobiology, 5, 401–411, doi:10.1111/j.1472-4669.2007.00117.x, 2007.

Brewer, P. G. and Spencer, D. W.: Colorimetric determination of manganese in anoxic waters, Limnol. Oceanogr., 16, 107–110, 1971.

Comte, S., Guibaud, G., and Baudu, M.: Relations between extraction protocols for activated sludge extracellular polymeric substances (EPS) and EPS complexation properties Part I. Comparison of the efficiency of eight EPS extraction methods, Enzyme Microb. Tech., 38, 237–245, doi:10.1016/j.enzmictec.2005.06.016, 2006.

Diem, D. and Stumm, W.: Is dissolved Mn^{2+} being oxidized by O_2 in absence of Mn-bacteria or surface catalysts, Geochim. Cosmochim. Ac., 48, 1571–1573, doi:10.1016/0016-7037(84)90413-7, 1984.

Duckworth, O. W. and Martin, S. T.: Role of molecular oxygen in the dissolution of siderite and rhodochrosite, Geochim. Cosmochim. Ac., 68, 607–621, doi:10.1016/S0016-7037(03)00464-2, 2004.

Fan, D. L. and Yang, P. J.: Introduction to and classification of manganese deposits of China, Ore Geol. Rev., 15, 1–13, doi:10.1016/S0169-1368(99)00011-6, 1999.

Fowler, T. A., Holmes, P. R., and Crundwell, F. K.: Mechanism of pyrite dissolution in the presence of Thiobacillus ferrooxidans, Appl. Environ. Microb., 65, 2987–2993, 1999.

Gehrke, T., Telegdi, J., Thierry, D., and Sand, W.: Importance of extracellular polymeric substances from Thiobacillus ferrooxidans for bioleaching, Appl. Environ. Microb., 64, 2743–2747, 1998.

Germann, K.: Deposition of Manganese and Iron Carbonates and Silicates in Liassic Marls of the Northern Limestone Alps (Kalkalpen), Int. Un. Geol. Sci., 3, 129–138, 1973.

BGD
11, 7273–7290, 2014

Guibaud, G., Tixier, N., Bouju, A., and Baudu, M.: Relation between extracellular polymers' composition and its ability to complex Cd, Cu and Pb, Chemosphere, 52, 1701–1710, doi:10.1016/S0045-6535(03)00355-2, 2003.
Guibaud, G., Comte, S., Bordas, F., Dupuy, S., and Baudu, M.: Comparison of the complexation potential of extracellular polymeric substances (EPS), extracted from activated sludges and produced by pure bacteria strains, for cadmium, lead and nickel, Chemosphere, 59, 629–638, doi:10.1016/j.chemosphere.2004.10.028, 2005.
Hansel, C. M., Zeiner, C. A., Santelli, C. M., and Webb, S. M.: Mn(II) oxidation by an ascomycete fungus is linked to superoxide production during asexual reproduction, P. Natl. Acad. Sci. USA, 109, 12621–12625, doi:10.1073/pnas.1203885109, 2012.
Jensen, D. L., Boddum, J. K., Tjell, J. C., and Christensen, T. H.: The solubility of rhodochrosite ($MnCO_3$) and siderite ($FeCO_3$) in anaerobic aquatic environments, Appl. Geochem., 17, 503–511, doi:10.1016/S0883-2927(01)00118-4, 2002.
Kim, D. G., Jiang, S., Jeong, K., and Ko, S. O.: Removal of 17 alpha-ethinylestradiol by biogenic manganese oxides produced by the *Pseudomonas putida* strain MnB1, Water Air Soil Poll., 223, 837–846, doi:10.1007/s11270-011-0906-6, 2012.
Lafferty, B. J., Ginder-Vogel, M., and Sparks, D. L.: Arsenite oxidation by a poorly crystalline manganese-oxide 1. Stirred-flow experiments, Environ Sci. Technol., 44, 8460–8466, doi:10.1021/Es102013p, 2010.
Learman, D. R., Voelker, B. M., Vazquez-Rodriguez, A. I., and Hansel, C. M.: Formation of manganese oxides by bacterially generated superoxide, Nat. Geosci., 4, 95–98, doi:10.1038/Ngeo1055, 2011a.
Learman, D. R., Wankel, S. D., Webb, S. M., Martinez, N., Madden, A. S., and Hansel, C. M.: Coupled biotic-abiotic Mn(II) oxidation pathway mediates the formation and structural evolution of biogenic Mn oxides, Geochim. Cosmochim. Ac., 75, 6048–6063, doi:10.1016/j.gca.2011.07.026, 2011b.
Luo, Y. X. and Millero, F. J.: Solubility of rhodochrosite ($MnCO_3$) in NaCl solutions, J. Solution Chem., 32, 405–416, doi:10.1023/A:1024568711020, 2003.
Madden, A. S. and Hochella, M. F.: A test of geochemical reactivity as a function of mineral size: manganese oxidation promoted by hematite nanoparticles, Geochim. Cosmochim. Ac., 69, 389–398, doi:10.1016/j.gca.2004.06.035, 2005.
Nara, M., Tasumi, M., Tanokura, M., Hiraoki, T., Yazawa, M., and Tsutsumi, A.: Infrared studies of interaction between metal-ions and Ca^{2+}-binding proteins – marker bands for identifying

BGD
11, 7273–7290, 2014

the types of coordination of the side-chain COO^- groups to metal-ions in pike parvalbumin (Pi = 4.10), Febs Lett., 349, 84–88, doi:10.1016/0014-5793(94)00645-8, 1994.
Okazaki, M., Sugita, T., Shimizu, M., Ohode, Y., Iwamoto, K., de Vrind de Jong, E. W., de Vrind, J. P. M., and Corstjens, P. L. A. M.: Partial purification and characterization of manganese-oxidizing factors of Pseudomonas fluorescens GB-1, Appl. Environ. Microb., 63, 4793–4799, 1997.
Okita, P. M.: Manganese carbonate mineralization in the Molango district, Mexico, Econ. Geol. Bull. Soc., 87, 1345–1366, 1992.
Omoike, A. and Chorover, J.: Spectroscopic study of extracellular polymeric substances from Bacillus subtilis: aqueous chemistry and adsorption effects, Biomacromolecules, 5, 1219–1230, doi:10.1021/Bm034461z, 2004.
Paxman, M. B. L. S.: Modification of the lowry procedure for the analysis of proteolipid protein, Anal. Biochem., 47, 184–192, 1972.
Rohwerder, T., Gehrke, T., Kinzler, K., and Sand, W.: Bioleaching review part A: Progress in bioleaching: fundamentals and mechanisms of bacterial metal sulfide oxidation, Appl. Microbiol. Biot., 63, 239–248, doi:10.1007/s00253-003-1448-7, 2003.
Roy, S.: Genetic diversity of manganese deposition in the terrestrial geological record, Geol. Soc. Spec. Publ., 119, 5–27, 1997.
Saha, S. K. and Brewer, C. F.: Determination of the concentrations of oligosaccharides, complex type carbohydrates, and glycoproteins using the phenol sulfuric-acid method, Carbohyd. Res., 254, 157–167, 1994.
Shiller, A. M. and Stephens, T. H.: Microbial manganese oxidation in the lower Mississippi River: methods and evidence, Geomicrobiol. J., 22, 117–125, doi:10.1080/01490450590945924, 2005.
Spiro, T. G., Bargar, J. R., Sposito, G., and Tebo, B. M.: Bacteriogenic manganese oxides, Accounts Chem. Res., 43, 2–9, doi:10.1021/Ar800232a, 2010.
Tang, Y. Z., Zeiner, C. A., Santelli, C. M., and Hansel, C. M.: Fungal oxidative dissolution of the Mn(II)-bearing mineral rhodochrosite and the role of metabolites in manganese oxide formation, Environ. Microbiol., 15, 1063–1077, doi:10.1111/1462-2920.12029, 2013.
Tebo, B. M., Johnson, H. A., McCarthy, J. K., and Templeton, A. S.: Geomicrobiology of manganese(II) oxidation, Trends Microbiol., 13, 421–428, doi:10.1016/j.tim.2005.07.009, 2005.
Tributsch, H.: Direct versus indirect bioleaching, Hydrometallurgy, 59, 177–185, doi:10.1016/S0304-386x(00)00181-X, 2001.

BGD
11, 7273–7290, 2014

Villalobos, M., Toner, B., Bargar, J., and Sposito, G.: Characterization of the manganese oxide produced by *Pseudomonas putida* strain MnB1, Geochim Cosmochim. Ac., 67, 2649–2662, doi:10.1016/S0016-7037(03)00217-5, 2003.

Zhang, D. Y., Lee, D. J., and Pan, X. L.: Desorption of Hg(II) and Sb(V) on extracellular polymeric substances: effects of pH, EDTA, Ca(II) and temperature shocks, Bioresource Technol., 128, 711–715, doi:10.1016/j.biortech.2012.10.089, 2013.

Zhu, M. Q., Paul, K. W., Kubicki, J. D., and Sparks, D. L.: Quantum chemical study of arsenic(III, V) adsorption on Mn-oxides: implications for arsenic(III) oxidation, Environ. Sci. Technol., 43, 6655–6661, doi:10.1021/Es900537e, 2009.

BGD
11, 7273–7290, 2014

Table 1. Dissolution rate of rhodochrosite under various conditions. Data were means ± standard error (n = 3) and significant levels between control and EPS treatments were indicated by asterisks ($p < 0.05$).

Exp. parameters	Mn dosages ($g\,L^{-1}$)	EPS con. ($mg\,TOC\,L^{-1}$)	Initial pH	Ionic strength (M)	Dissolution rates ($\mu g\,Mn(II)\,min^{-1}$)
Initial pH	5	0	5.0	0.01	0.101 ± 0.001
	5	0.8	5.0	0.01	0.768 ± 0.181*
	5	0	7.0	0.01	0.055 ± 0.003
	5	0.8	7.0	0.01	0.106 ± 0.016*
	5	0	8.0	0.01	0.047 ± 0.004
	5	0.8	8.0	0.01	0.028 ± 0.015
Ionic strength	5	0	7.0	0.01	0.055 ± 0.003
	5	0.8	7.0	0.01	0.106 ± 0.016*
	5	0	7.0	0.1	0.081 ± 0.005
	5	0.8	7.0	0.1	0.141 ± 0.009*
	5	0	7.0	0.5	0.111 ± 0.005
	5	0.8	7.0	0.5	0.163 ± 0.002*
EPS concentration	5	0	7.0	0.01	0.055 ± 0.003
	5	0.4	7.0	0.01	0.075 ± 0.003*
	5	0.8	7.0	0.01	0.106 ± 0.016*
	5	1.6	7.0	0.01	0.111 ± 0.018*
Rhodochrosite dosage	2	0	7.0	0.01	0.059 ± 0.004
	2	0.8	7.0	0.01	0.088 ± 0.007*
	5	0	7.0	0.01	0.055 ± 0.003
	5	0.8	7.0	0.01	0.106 ± 0.016*
	10	0	7.0	0.01	0.057 ± 0.001
	10	0.8	7.0	0.01	0.107 ± 0.011*

BGD
11, 7273–7290, 2014

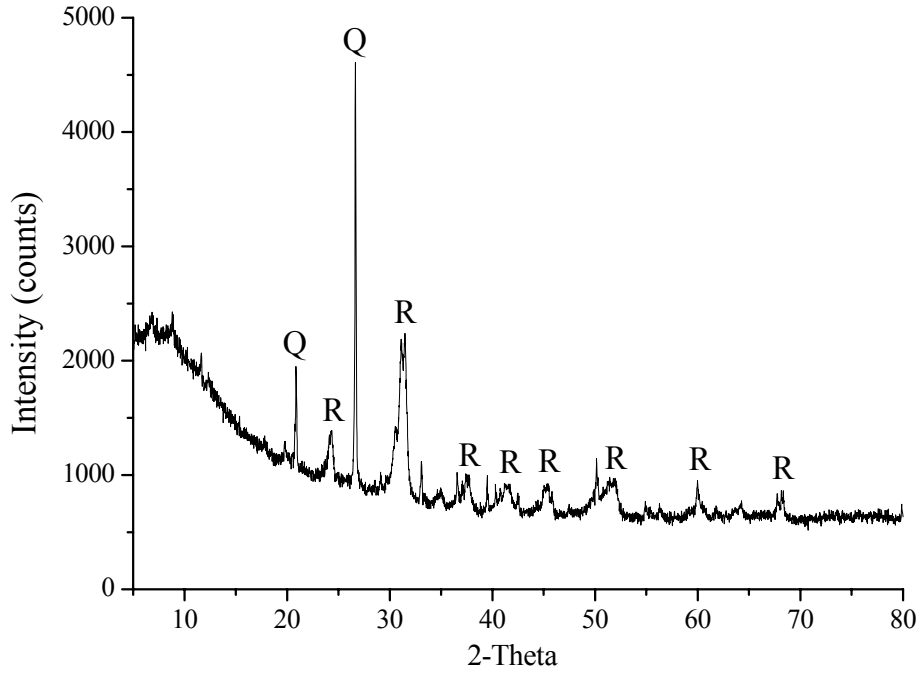

Figure 1. XRD patterns of natural Rhodochrosite (R, Rhodochrosite; Q, Quartz).

BGD
11, 7273–7290, 2014

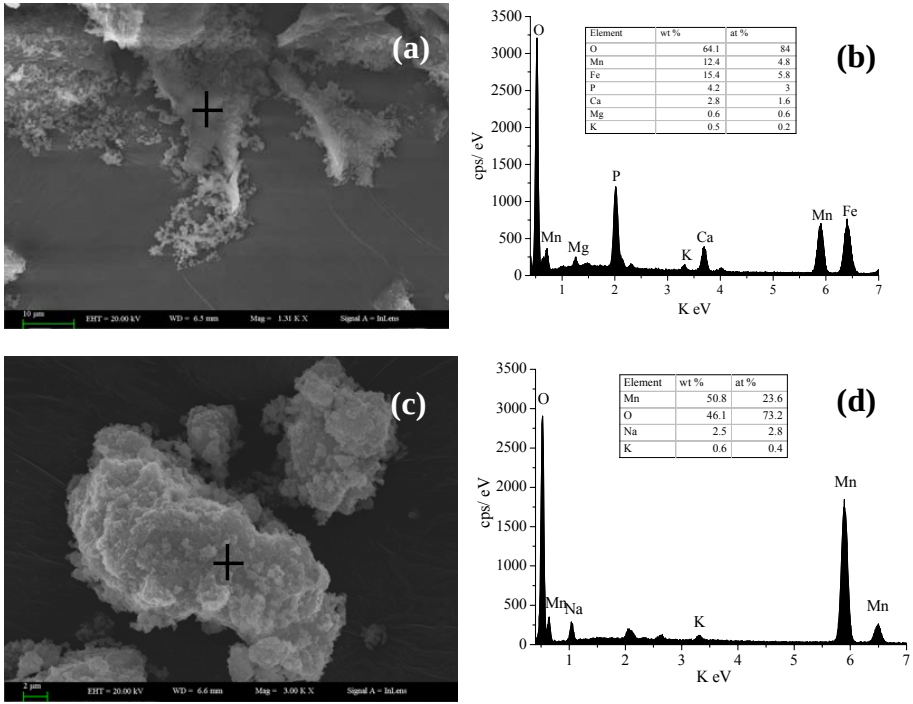

Figure 2. SEM and EDS spectra of biogenic Mn oxides **(a, b)** and freshly synthetic δ-MnO_2 **(c, d).**

BGD
11, 7273–7290, 2014

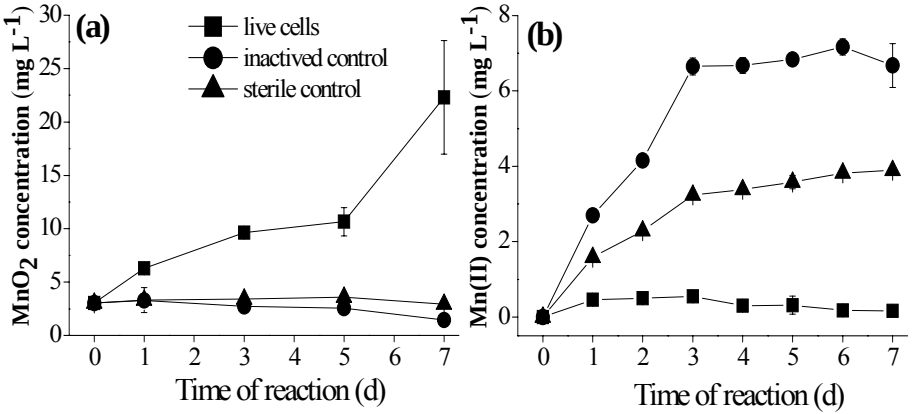

Figure 3. Variation of Mn oxides **(a)** and Mn(II) concentration **(b)** as a function of reaction time during the dissolution of natural rhodochrosite.

BGD
11, 7273–7290, 2014

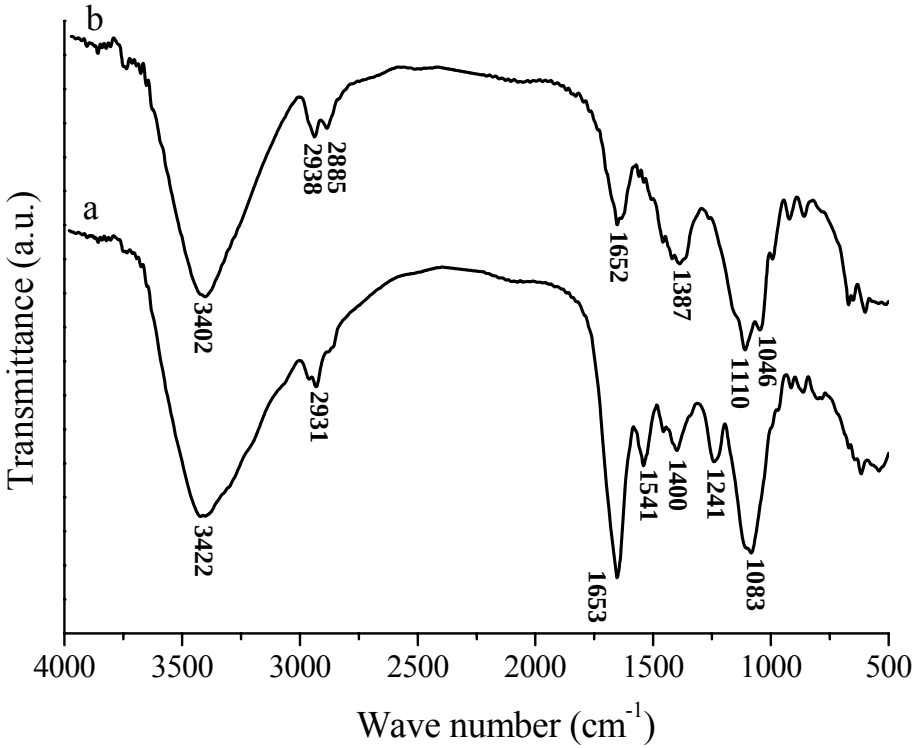

Figure 4. Comparsion of FTIR spectra of EPS before and after reaction with natural rhodochrosite: **(a)** Pristine EPS; **(b)** EPS after reaction with natural rhodochrosite.

BGD
11, 7273–7290, 2014